Exotic nuclei at low and high spins in covariant density functional theory

Anatoli Afanasjev

Mississippi State University (MSU), USA

1. **Motivation and framework**
2. **Hyperheavy (Z>126) nuclei: from ellipsoidal to toroidal shapes**
3. **Rotation in exotic very proton and neutron-rich nuclei: new mechanisms leading to extension of nuclear landscape.**
4. **Conclusions**

In collaboration with S.E. Agbemava (MSU, now FRIB), A. Taninah, S. Teeti, D. Ray (all MSU) and N. Itagaki (Osaka Metropolitan U.)

Collective degrees of freedom (deformation, rotation, fission)

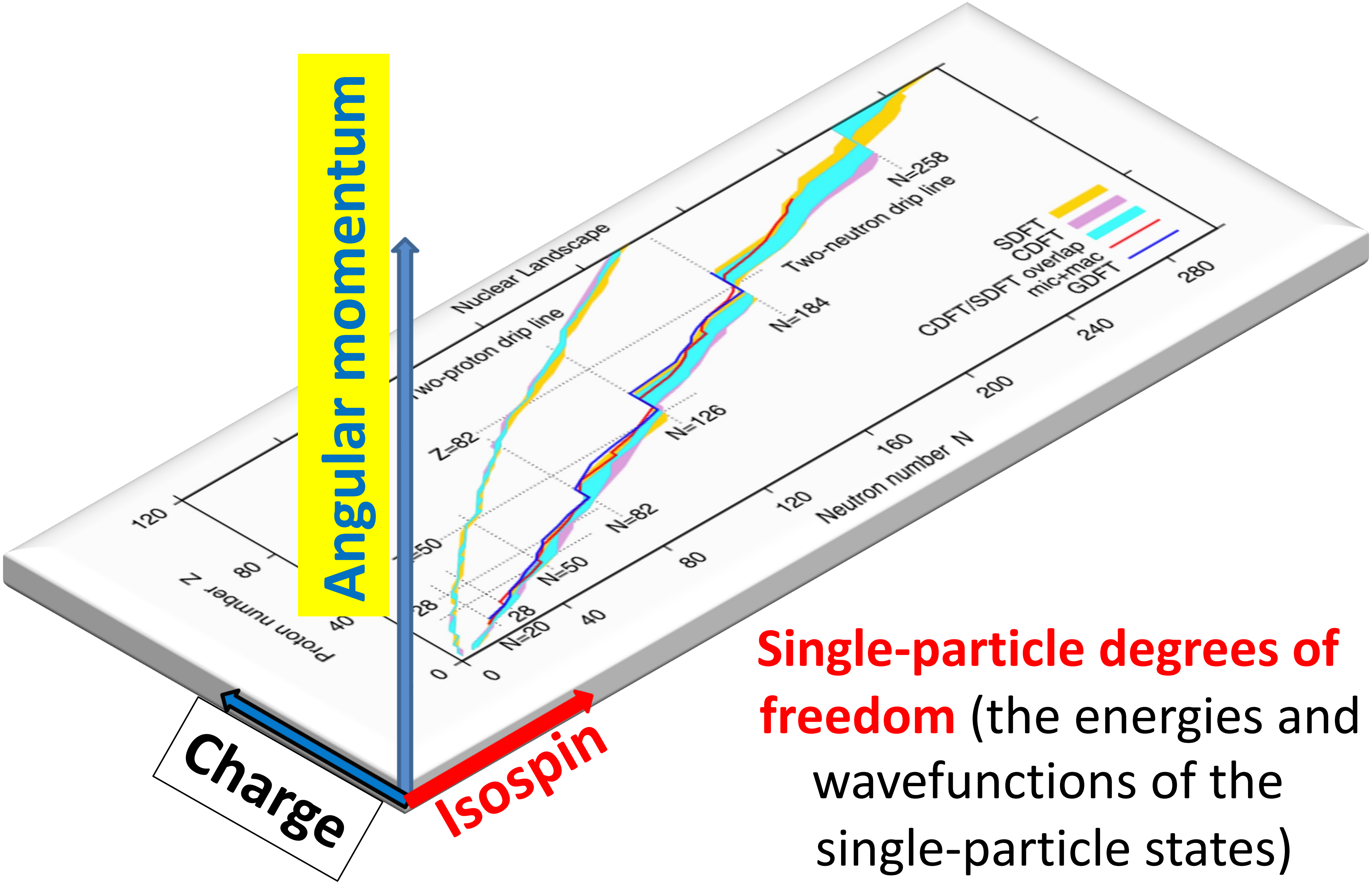

Single-particle degrees of freedom (the energies and wavefunctions of the single-particle states)

Covariant density functional theory (CDFT)

The nucleons interact via the exchange of effective mesons →
→ **effective Lagrangian**

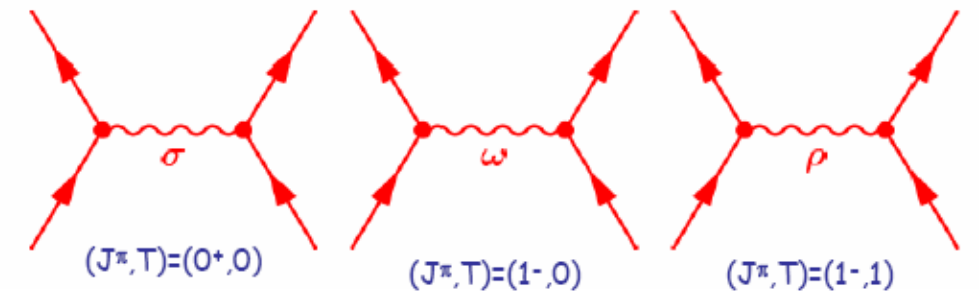

Long-range attractive scalar field

Short-range repulsive vector field

Isovector field

$$E_{\mathrm{RMF}}[\hat{\rho}, \phi_m] = \mathrm{Tr}[(\boldsymbol{\alpha p} + \beta m)\hat{\rho}] \pm \int \left[\frac{1}{2}(\nabla\phi_m)^2 + U(\phi_m)\right] \mathrm{d}^3 r + \mathrm{Tr}[(\Gamma_m \phi_m)\hat{\rho}]$$

density matrix $\hat{\rho}$

$\phi_m \equiv \{\sigma, \omega^\mu, \vec{\rho}^\mu, A^\mu\}$ - meson fields

$$\hat{h} = \frac{\delta E}{\delta \hat{\rho}}$$

Mean field

$$\hat{h}|\varphi_i\rangle = \varepsilon_i |\varphi_i\rangle$$

Eigenfunctions

Dirac equation for fermions

$$\{\vec{\alpha}\vec{p} + V + \beta(m + S)\}\,\Psi_i = \epsilon_i \Psi_i$$

$$\Psi_i = \begin{pmatrix} f_i(r) \\ i g_i(r) \end{pmatrix} = \begin{pmatrix} \text{large components} \\ \text{small components} \end{pmatrix}$$

Klein-Gordon equations for mesons

$$\{-\Delta + m_\sigma^2\}\,\sigma = -g_\sigma \rho_s - g_2 \sigma^2 - g_3 \sigma^3$$

$$\{-\Delta + m_\omega^2\}\,\omega_0 = g_\omega \rho_v$$

V ~ 350 MeV/nucleon
S ~ - 400 MeV/nucleon
U ~ - 50 MeV/nucleon

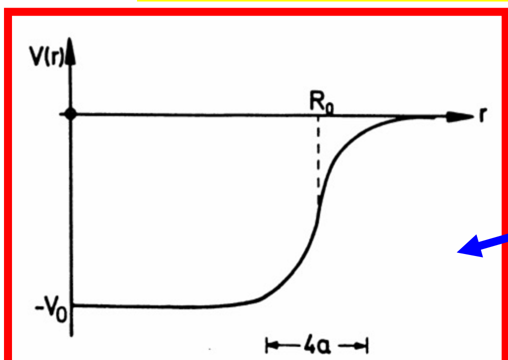

U=S+V

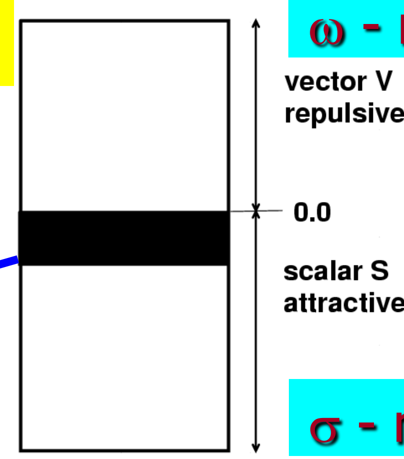

ω - meson

σ - meson

Densities

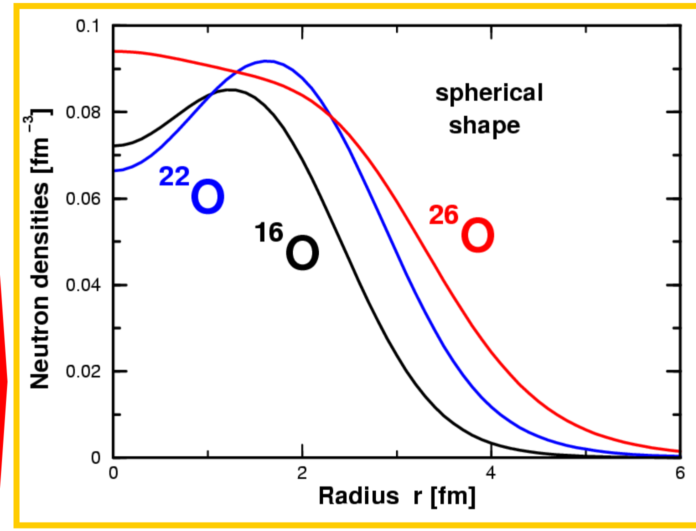

Single-particle energies

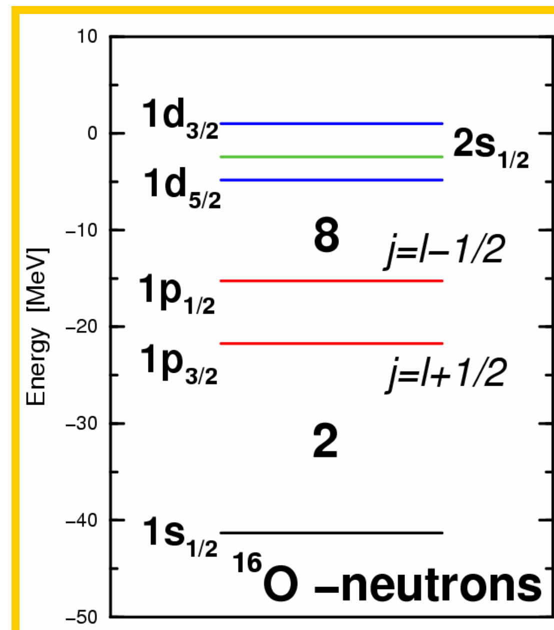

Relativistic Hartree-Bogoliubov (RHB) framework

$$\begin{pmatrix} h_D - \lambda & \Delta \\ -\Delta^* & -h_D^* + \lambda \end{pmatrix} \begin{pmatrix} U \\ V \end{pmatrix}_k = E_k \begin{pmatrix} U \\ V \end{pmatrix}_k$$

The separable version of the finite range Brink-Booker part of the Gogny D1S force is used in the particle-particle channel

$$V(\boldsymbol{r}_1, \boldsymbol{r}_2, \boldsymbol{r}_1', \boldsymbol{r}_2') = \\ = -f\, G\delta(\boldsymbol{R} - \boldsymbol{R}')P(r)P(r')\frac{1}{2}(1 - P^\sigma)$$

The NL3*, PC-PK1, DD-ME2, DD-PC1 and DD-MEδ covariant energy density functionals are used in order to assess the dependence of results on the functional and underlying single-particle structure and assess systematic theoretical uncertainties

The global results for even-even nuclei are available in tabulated form at:

S. Agbemava, AA, D, Ray, P.Ring, PRC **89**, 054320 (2014)
includes complete DD-PC1 mass table as supplement

Mass Explorer at FRIB (the results for DD-PC1, NL3*, DD-ME2, and DD-MEδ)
http://massexplorer.frib.msu.edu/content/DFTMassTables.html

A.V.Afanasjev, P.Ring, J. Konig, PRC 60 (1999) R051303, Nucl. Phys. A 676(2000) 196

Cranked Relativistic Hartree-Bogoliubov Theory

The CRHB equations for the fermions in the rotating frame in the one-dimensional cranking approximation

$$\begin{pmatrix} h_D - \lambda - \Omega_x \hat{J}_x & \hat{\Delta} \\ -\hat{\Delta}^* & -h_D^* + \lambda + \Omega_x \hat{J}_x \end{pmatrix} \begin{pmatrix} U_k \\ V_k \end{pmatrix} = E_k \begin{pmatrix} U_k \\ V_k \end{pmatrix}$$

Coriolis term

Klein-Gordon equations

$$\begin{aligned} \left\{-\Delta - (\Omega_x \hat{L}_x)^2 + m_\sigma^2\right\} \sigma(\boldsymbol{r}) &= -g_\sigma \rho_s(\boldsymbol{r}) - g_2 \sigma^2(\boldsymbol{r}) - g_3 \sigma^3(\boldsymbol{r}) \\ \left\{-\Delta - (\Omega_x \hat{L}_x)^2 + m_\omega^2\right\} \omega_0(\boldsymbol{r}) &= g_\omega \rho_v^{is}(\boldsymbol{r}) \\ \left\{-\Delta - (\Omega_x (\hat{L}_x + \hat{S}_x))^2 + m_\omega^2\right\} \boldsymbol{\omega}(\boldsymbol{r}) &= g_\omega \boldsymbol{j}^{is}(\boldsymbol{r}) \end{aligned}$$

Space-like components of vector mesons

currents

Important in rotating nuclei: give ~ 20-30% contr. to moments of inertia

Hyperheavy (Z>126) nuclei: from ellipsoidal to toroidal shapes

Agbemava, AA, Taninah, Gyawali,
PLB 782, 533 (2018)
PRC 99, 034316 (2019)
PRC 103, 034323 (2021)
Acta Phys. Polonica B, 13, 347 (2020)

Deformation energy curve of the $^{466}156$ nucleus in axial RHB calculations

The density profiles reflect their relative sizes with respect of the spherical shape in the minimum D.

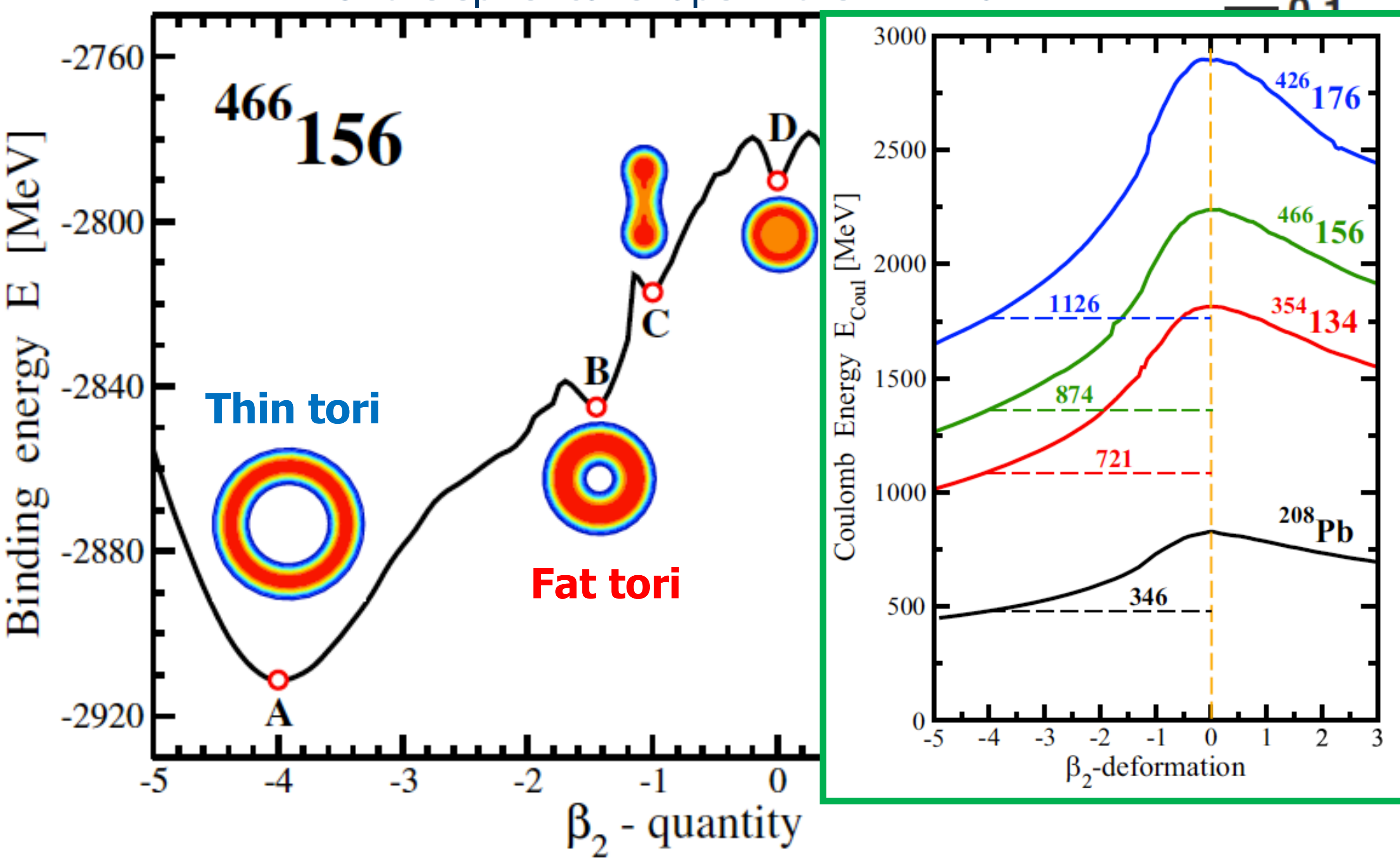

Extension of nuclear landscape to hyperheavy (Z>126) nuclei

Extension of proton drip line for ellipsoidal shapes

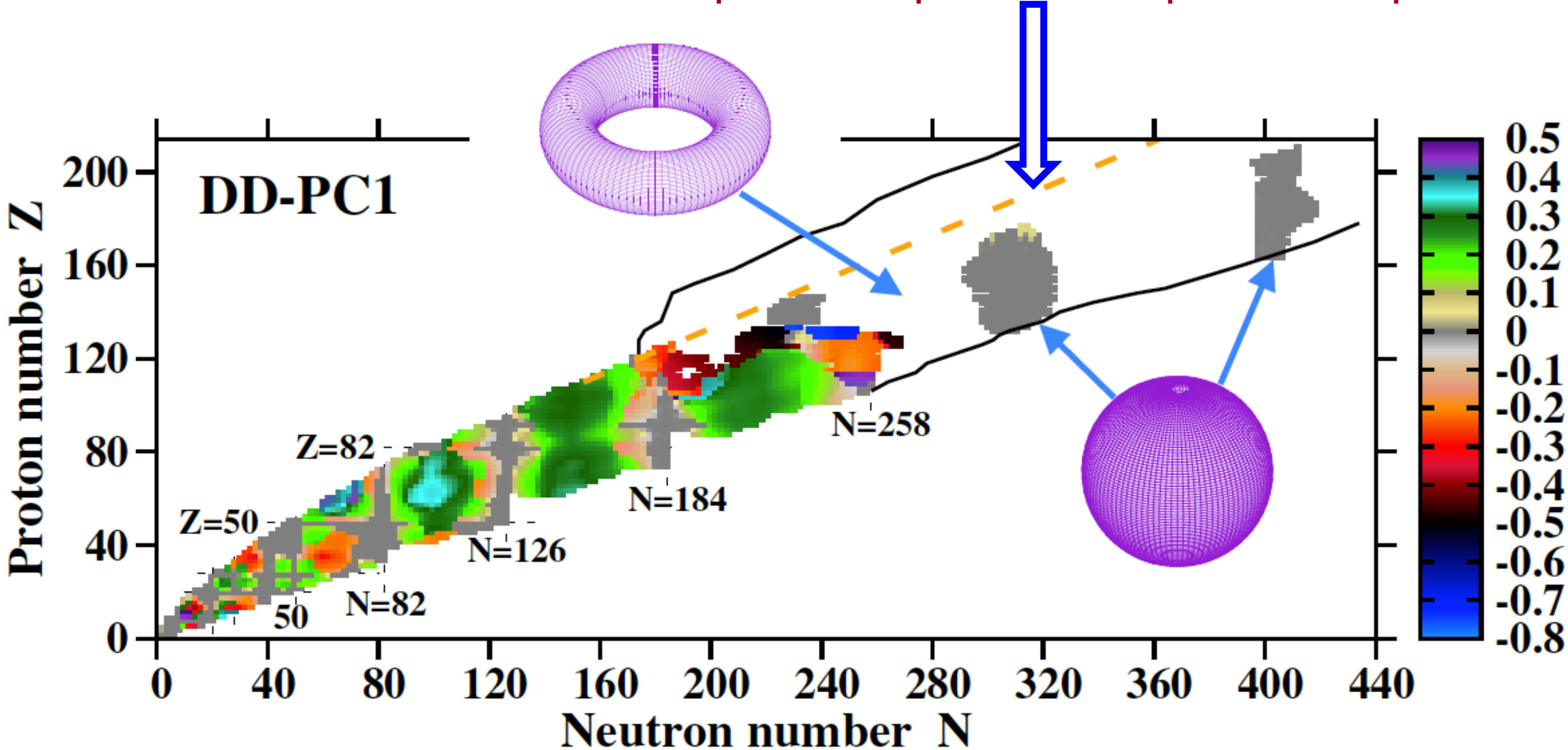

Agbemava, AA, Taninah, Gyawali,
PRC 99, 034316 (2019)
PLB 782, 533 (2018)
PRC 103, 034323 (2021)

Toroidal nuclei: the origin of the shift of two-proton drip line to more proton-rich nuclei

AA, S.E.Agbemava, A.Taninah
Acta Phys. Polonica B, 13, 347 (2020)

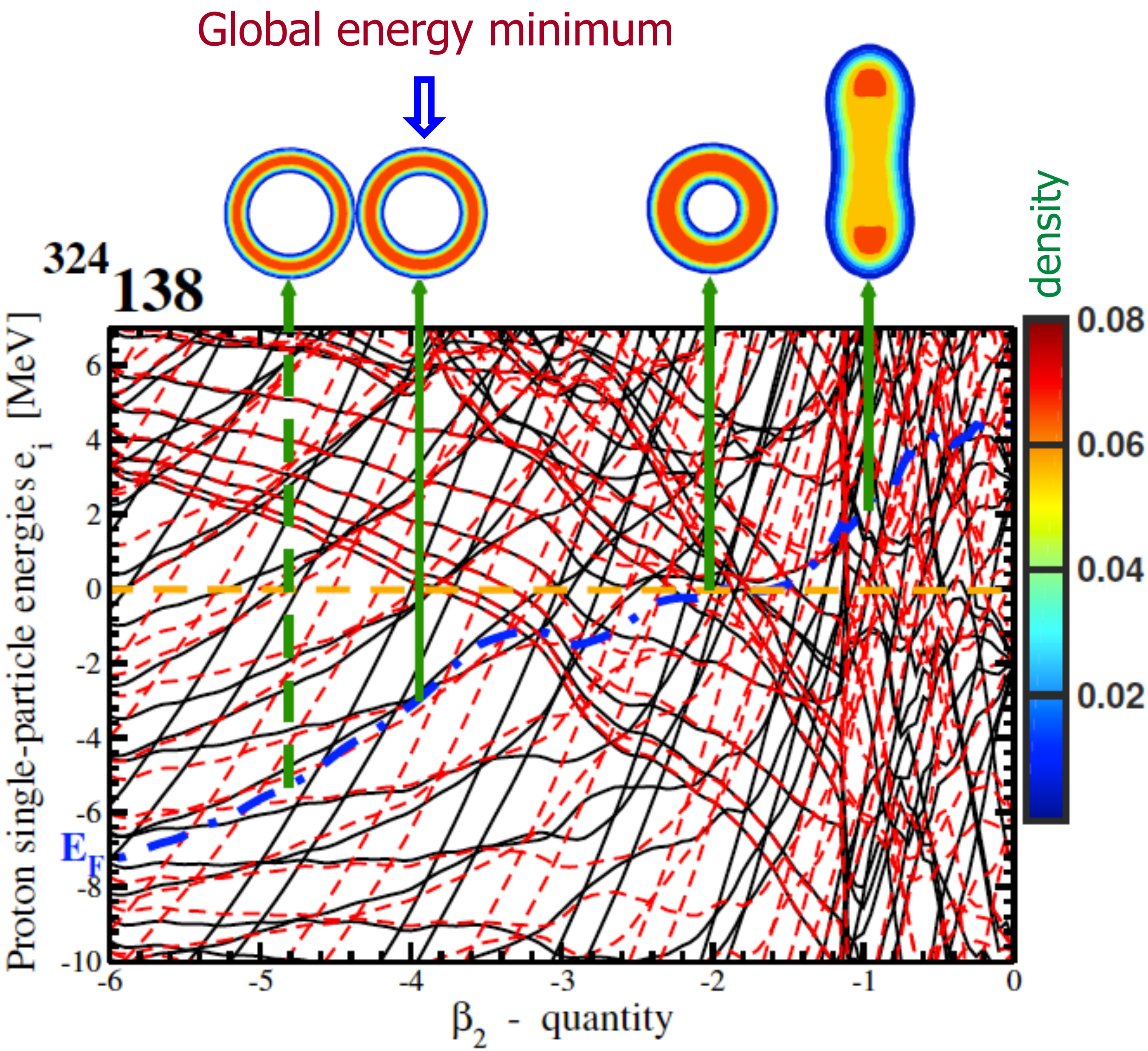

Fission barrier heights around "excited" spherical minimum

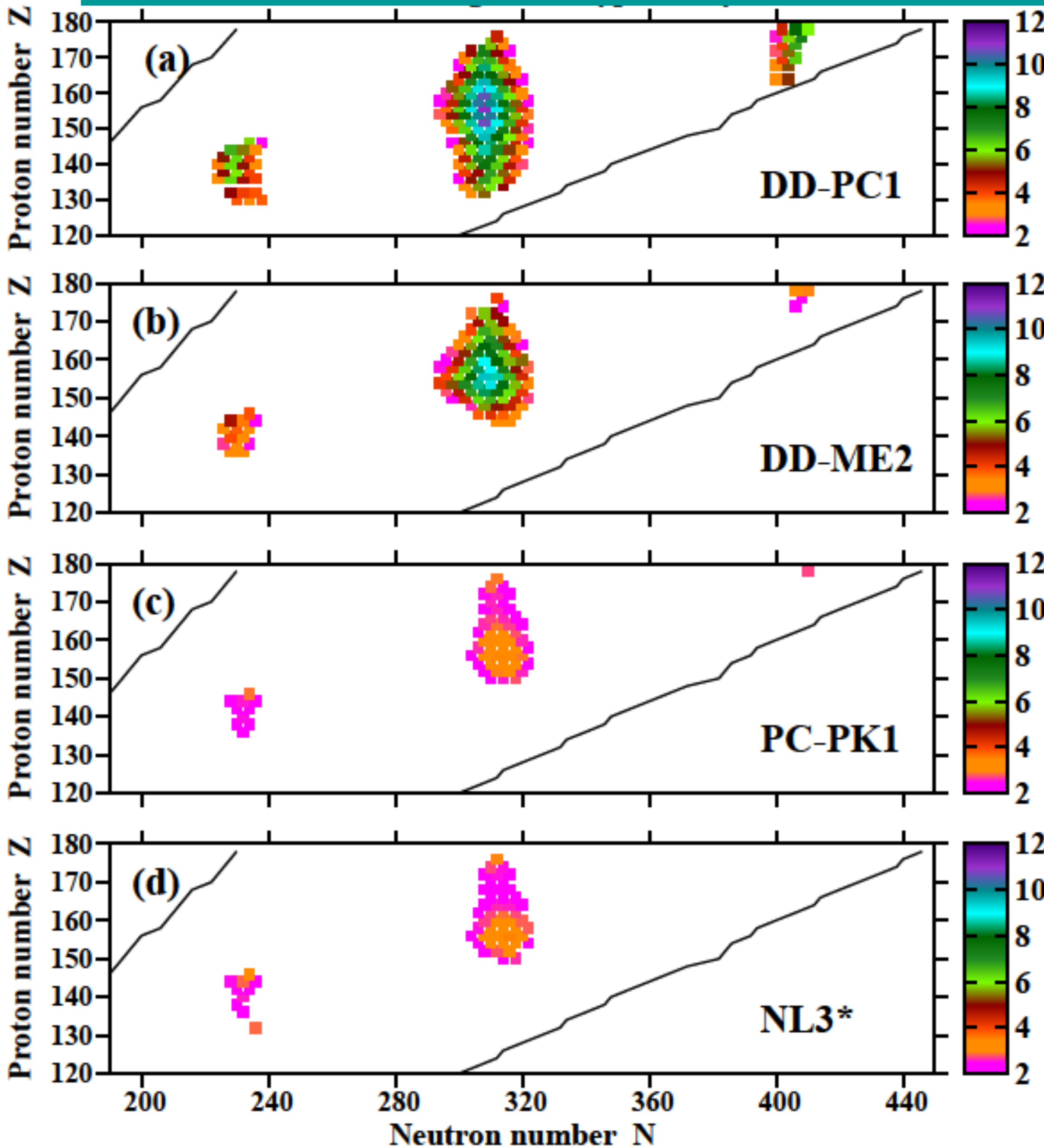

For the first time, we demonstrate the existence of three regions of spherical hyperheavy nuclei centered around **(Z~138, N~230)**, **(Z~156, N~310)** and **(Z~186, N~ 406)** which are expected to be relatively stable against spontaneous fission.

Neither octupole nor triaxial distortions significantly affect their stability

The toroidal shapes: distribution in nuclear chart and their stability with respect of breathing deformations

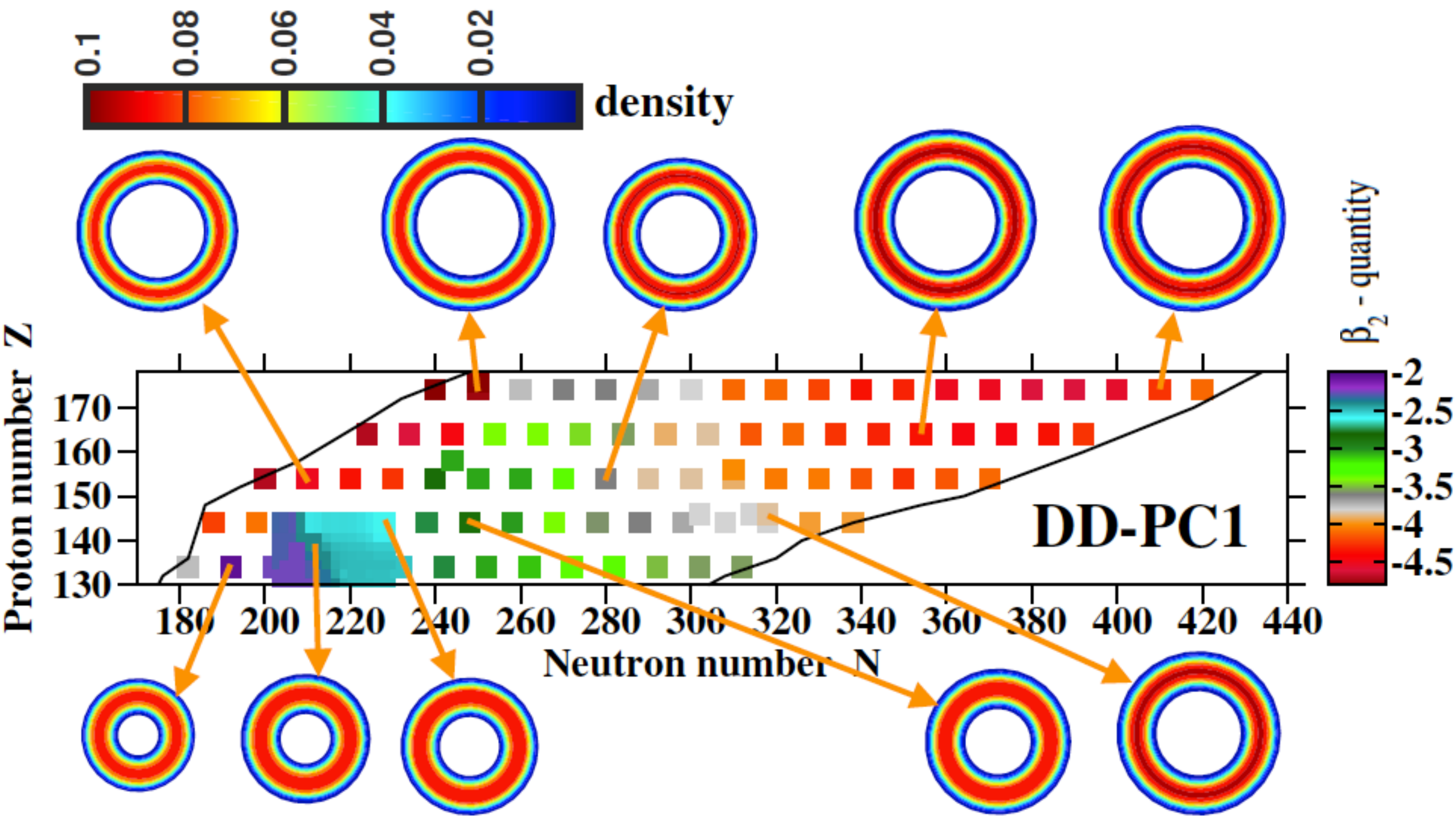

Toroidal nuclei are stable with respect of breathing deformations

The potential instabilities of toroidal shapes with respect of breathing deformations [shrinking instabilities]

From B.D.Texier et al, Inertial collapse of liquid rings, J. Fluid. Mech 717, R3 (2013)

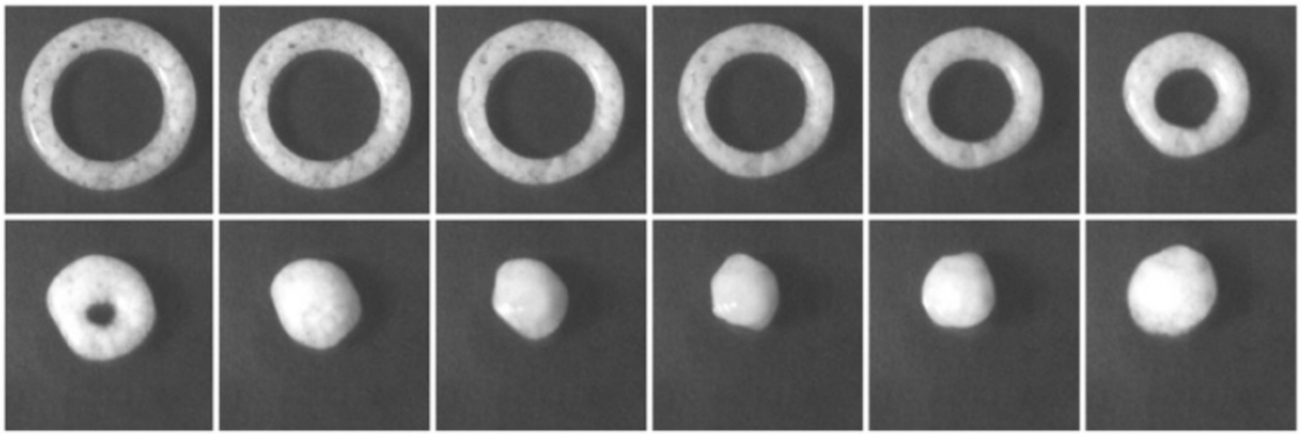

Fluid mechanics: Plateau-Rayleigh instabilities

Shrinking instabilities

FIGURE 3. Top view of a collapsing liquid oxygen ring, of initial inner radius $R_o = 4$ mm and initial width $a_o = 2$ mm. Time inter
available as a supplemental material a

Because of being charged systems toroidal nuclei are stable with respect of breathing deformations

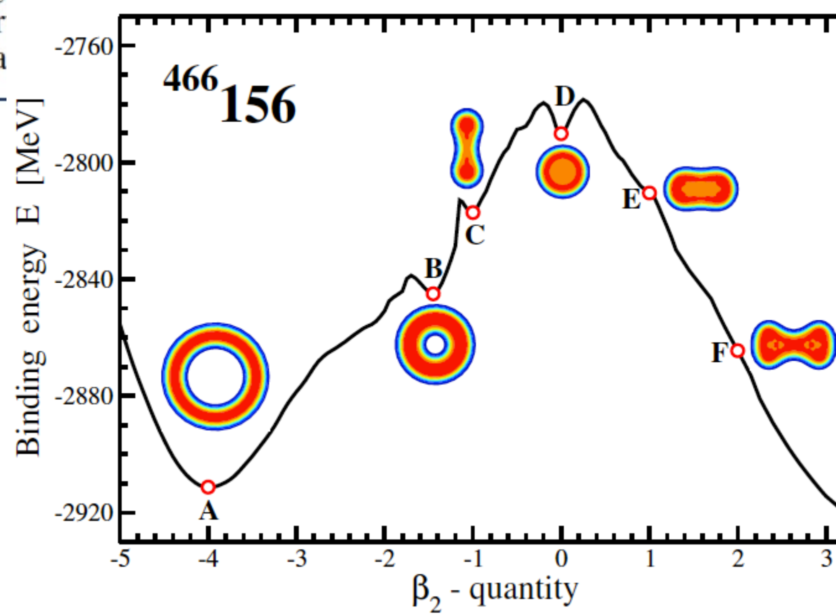

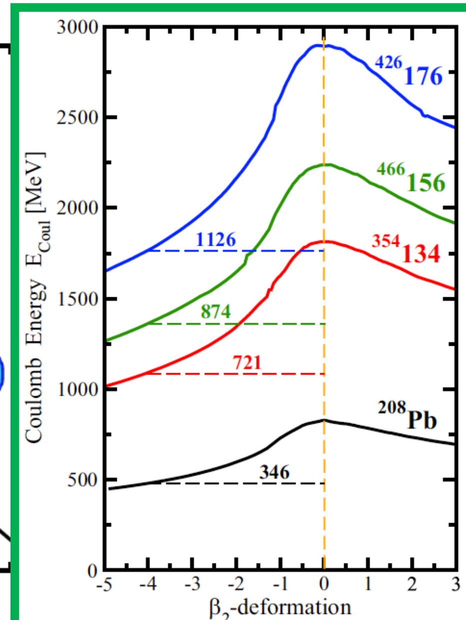

The potential instabilities of toroidal shapes with respect of sausage deformations.

From J.D.McGraw et al, Plateau-Rayleigh instability in a torus: formation and breakup of a polymer ring, Soft. Matter 6, 1258, (2010)

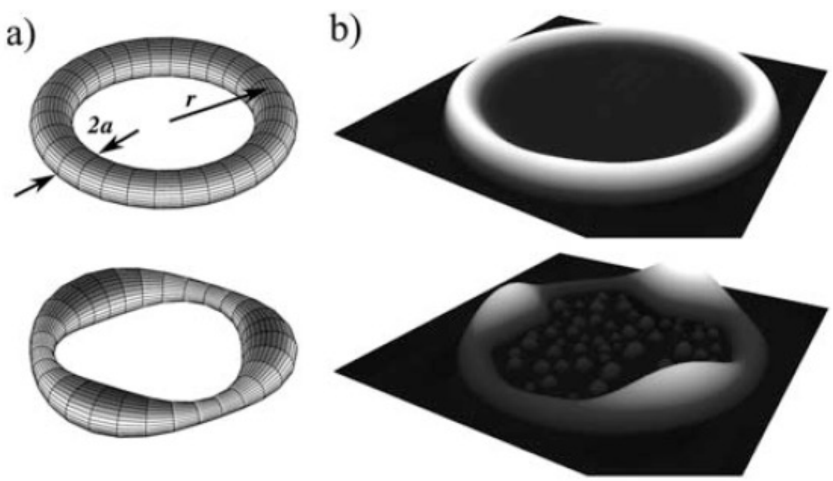

Fluid mechanics: Plateau-Rayleigh instabilities

Experiment: AFM topography images

In nuclear physics, this type of instability is called the instability with respect of sausage deformations (leads to multifragmentation)

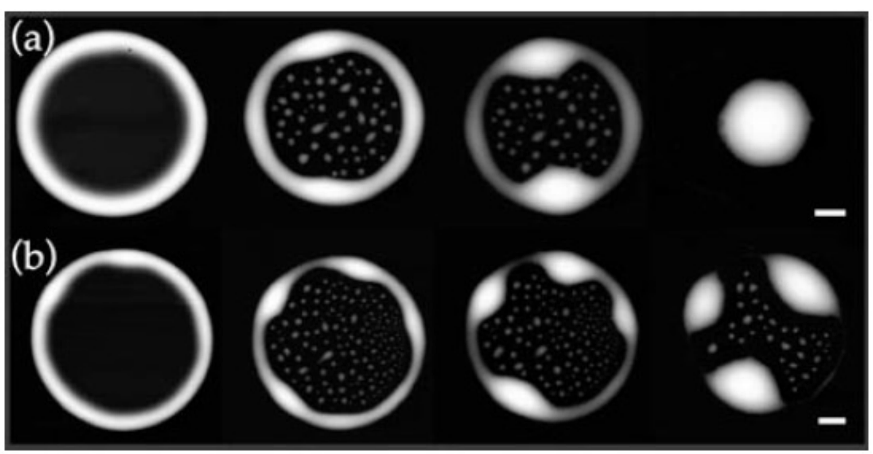

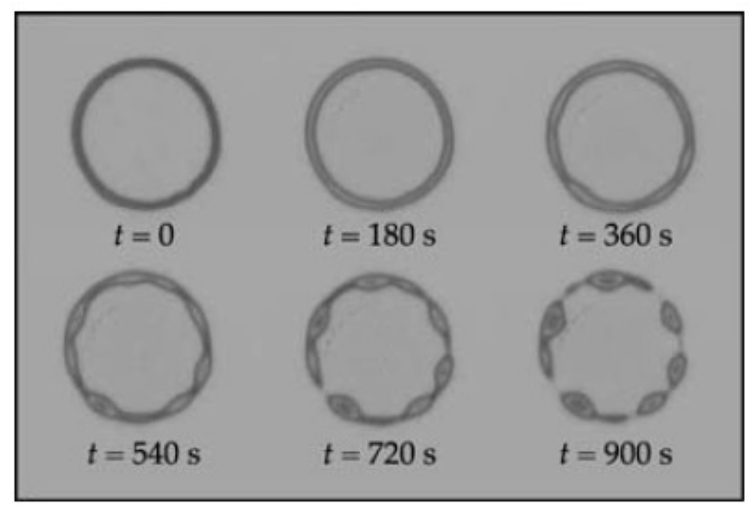

The potential stability of toroidal shapes with $\beta_2 \sim -2.5$ and $\beta_4 > 0$ in high-Z systems

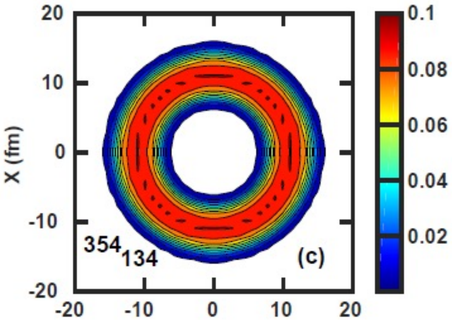

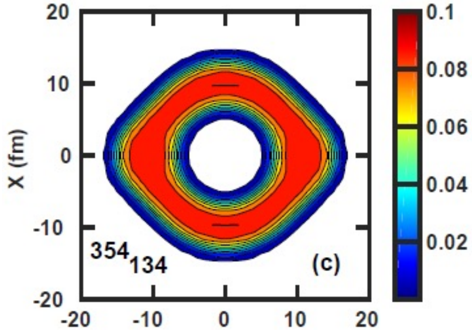

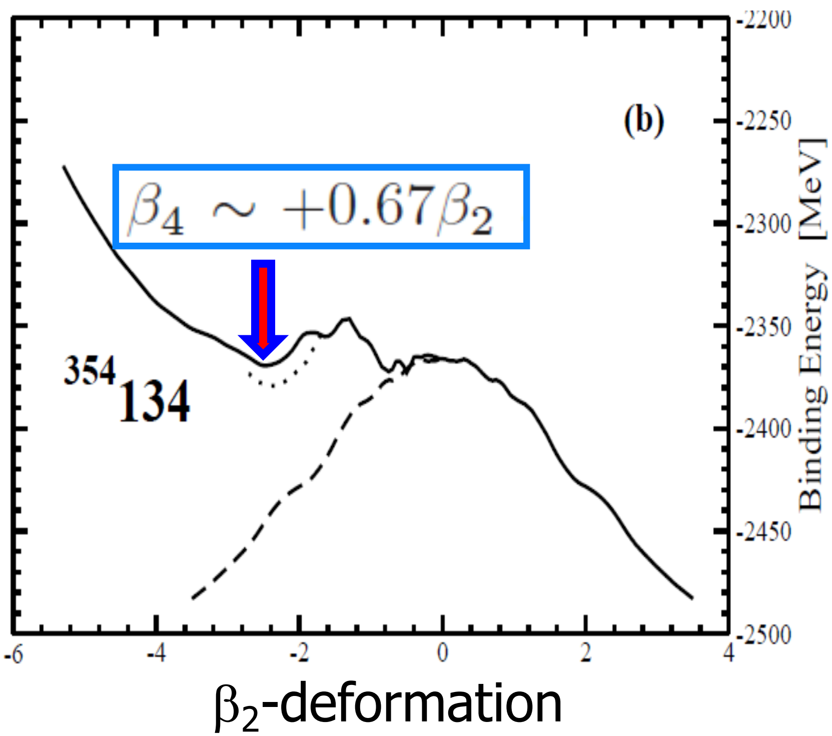

Fission barrier at E=4.2 MeV

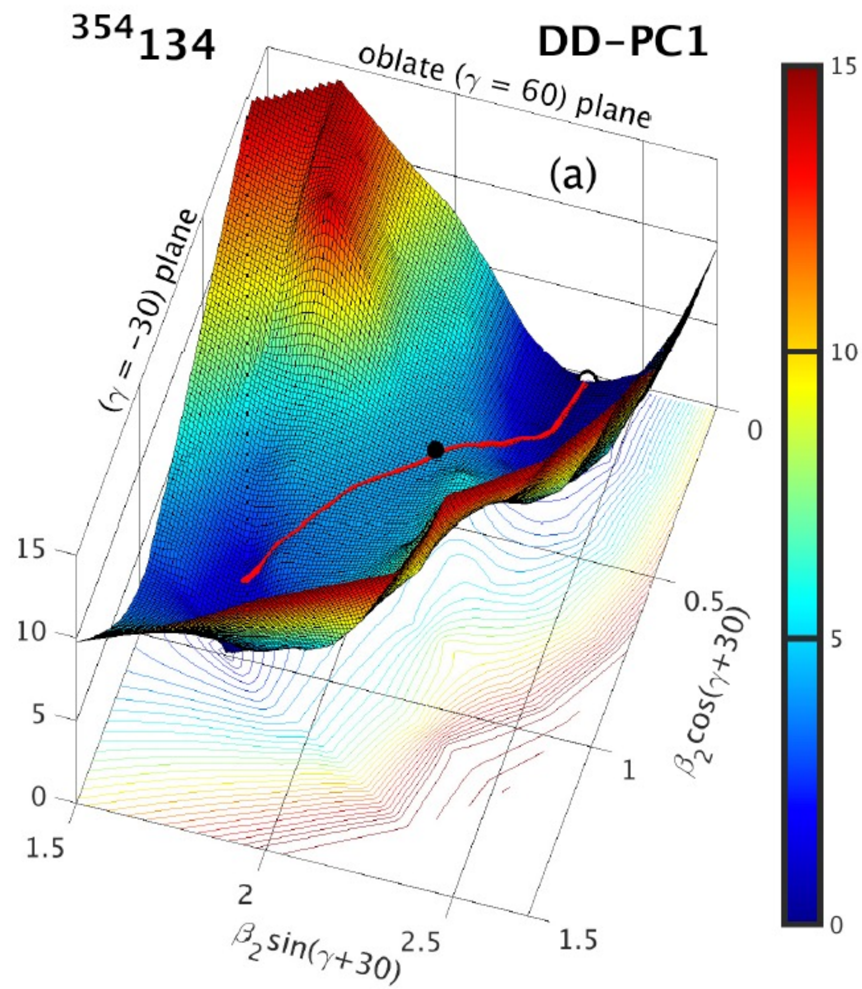

Fission barrier at E=8.5 MeV in the $^{348}138$ nucleus

Shell structure of toroidal shapes in the $^{348}138$ nucleus

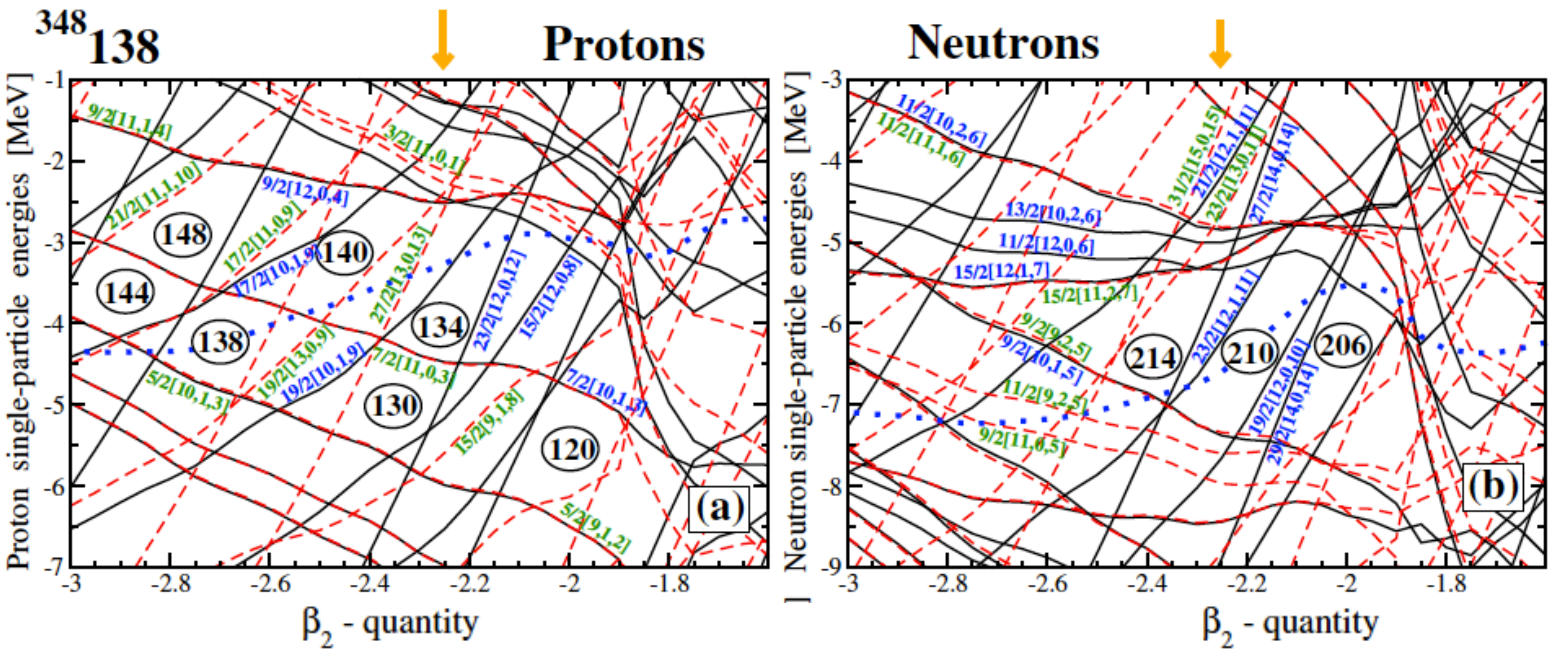

Orange arrow – the position of the minimum in potential energy curve

Single-particle states: solid black lines – positive parity

dashed red lines – negative parity

Large shell gap at N=210 and low density of the single-particle states in the vicinity of the Z=134-140 explain the stability of toroidal shapes with respect to even-multipole sausage deformations

Possible observation of toroidal shapes at high spin in ^{28}Si

X.G.Cao et al, PRC 99, 014606 (2019)

Examination of evidence for resonances at high excitation energy in the 7α disassembly of ^{28}Si

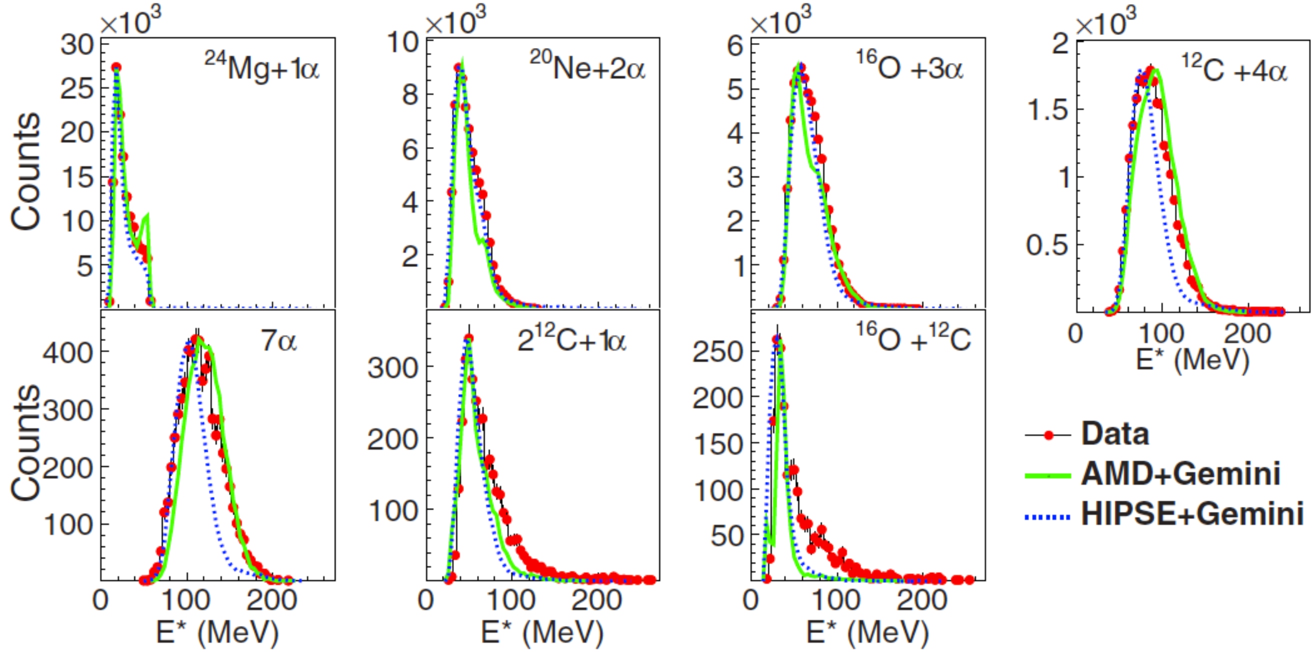

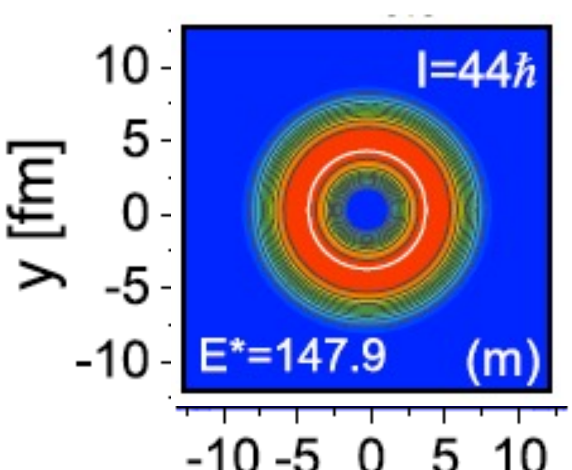

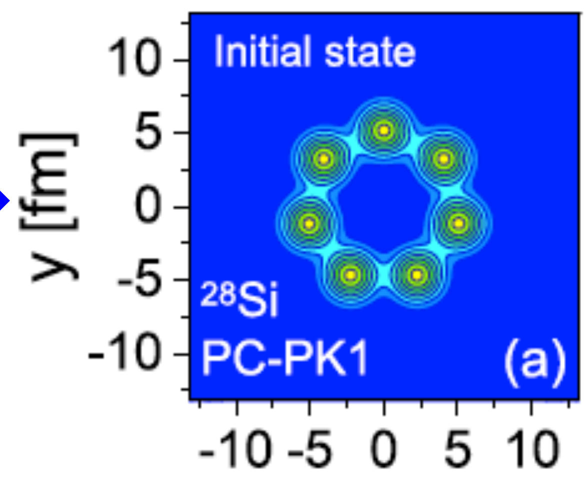

Z.X.Ren et al, NPA 996, 121696 (2020)

Going beyond known boundaries: rotation in very proton- and neutron-rich nuclei

The origin of new phenomenon:
the birth of particle-bound rotational bands
in neutron-rich nuclei

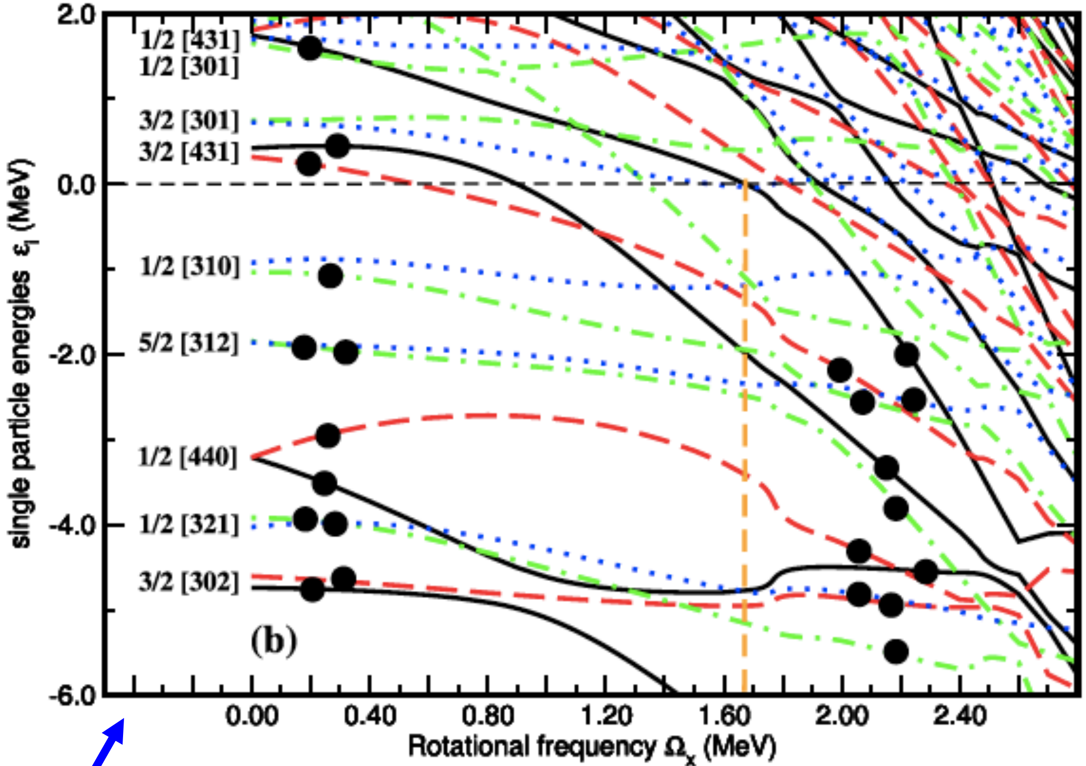

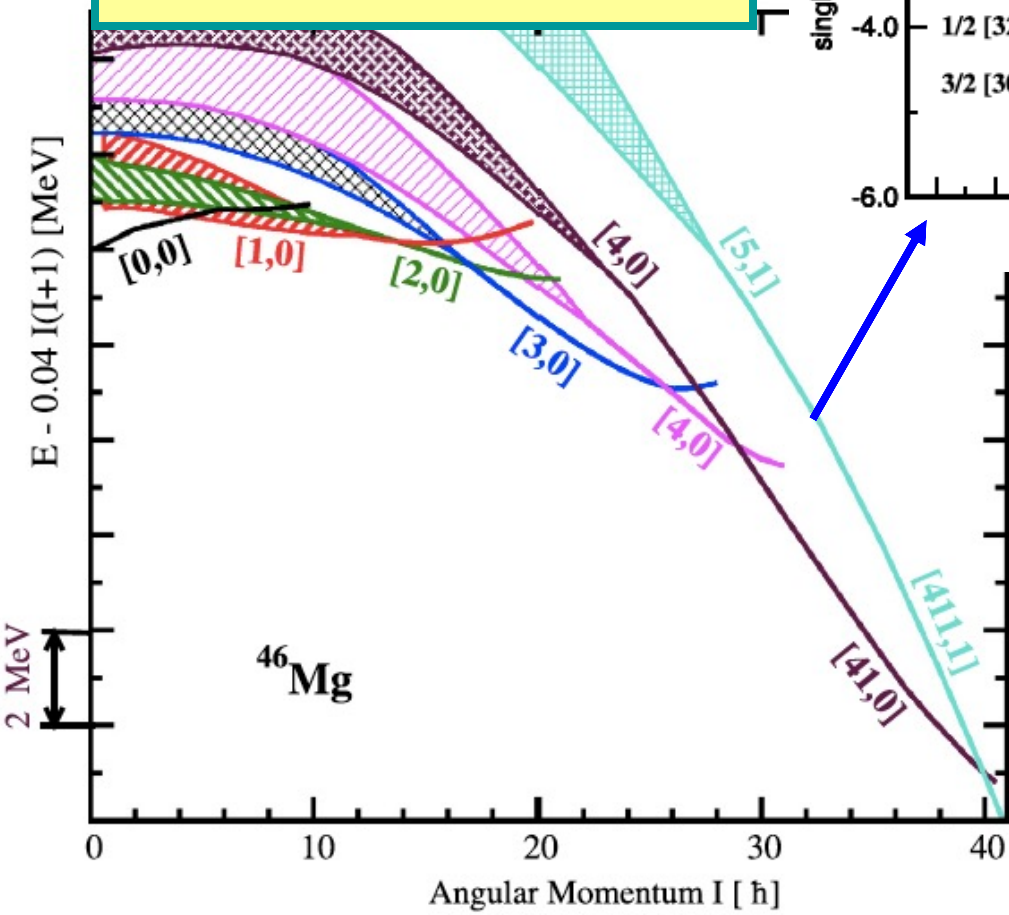

Cranked relativistic mean field calculations

AA, N. Itagaki, D. Ray, PLB 794 (2019) 7

Particle-hole excitations:
The tool for creation of new type of rotational bands consisting of resonance and particle-bound parts

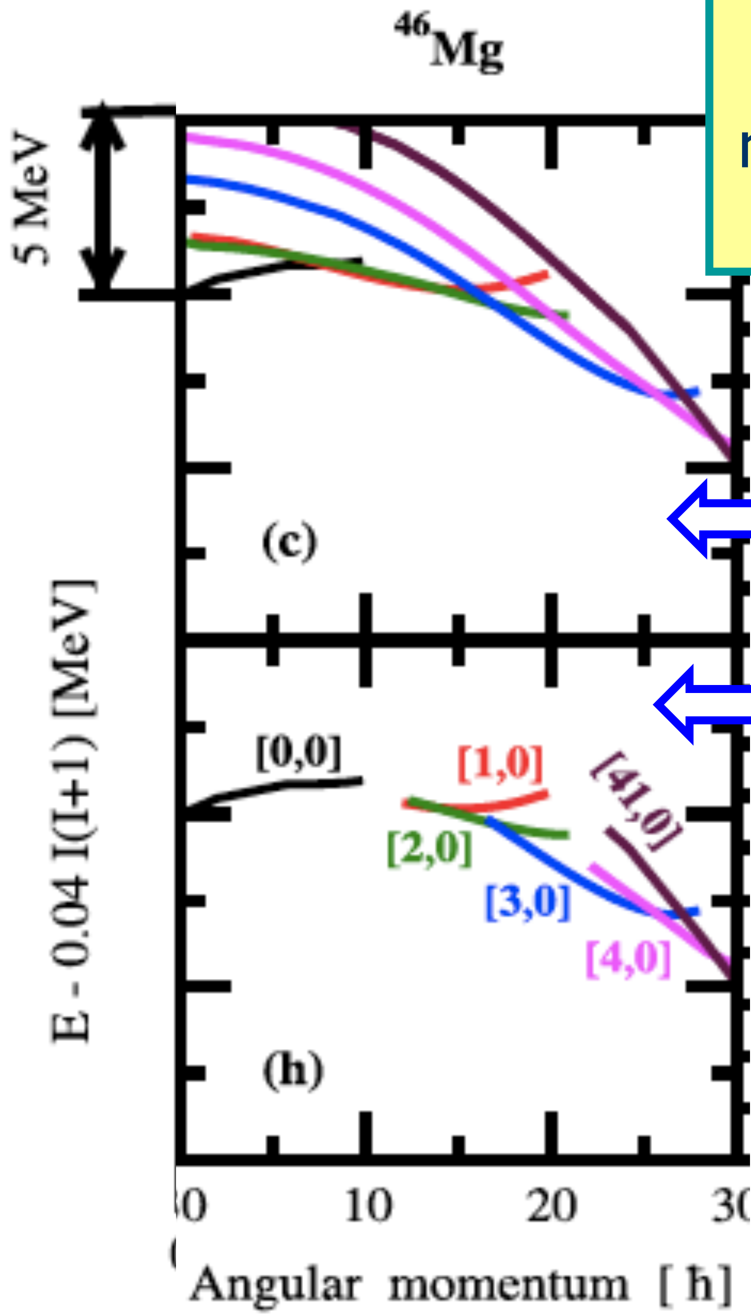

Resonance + particle-bound parts of bands are included. !!! Proper description of resonance parts requires the treatment of pairing in continuum

Only particle-bound parts of the bands are included. Fast rotation and multiply particle-hole excitations are expected to kill static pairing and thus the coupling with continuum.

^{46}Mg - last neutron bound nucleus at spin I=0 => defines spin zero neutron drip line

AA, N. Itagaki, D. Ray, PLB 794 (2019) 7

New phenomenon: the birth of particle-bound rotational bands in neutron-rich nuclei

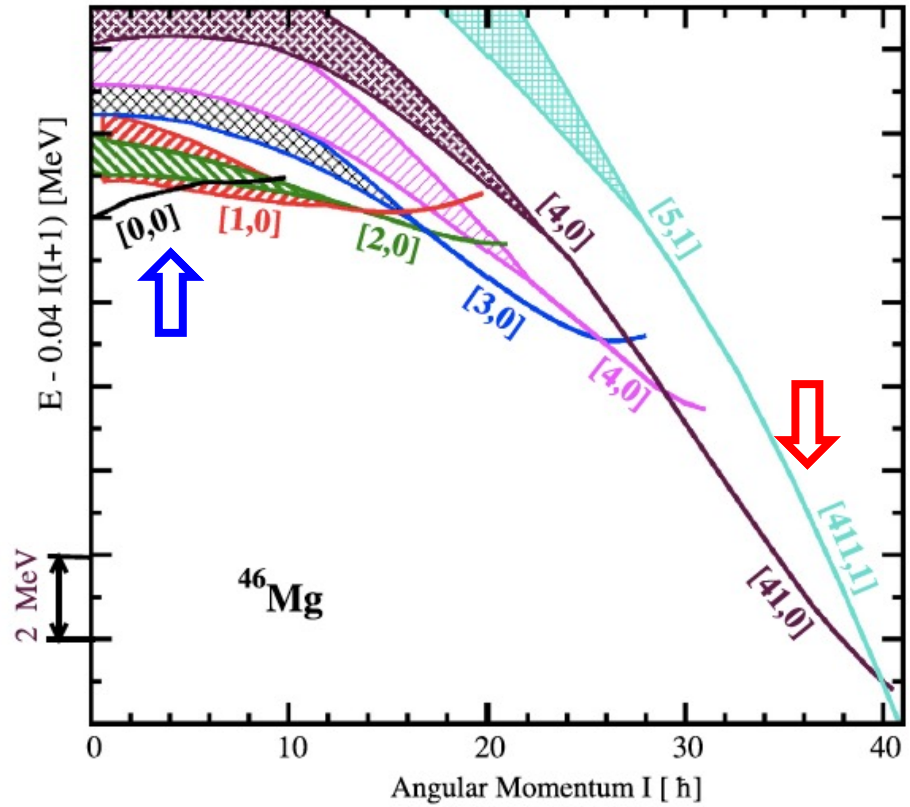

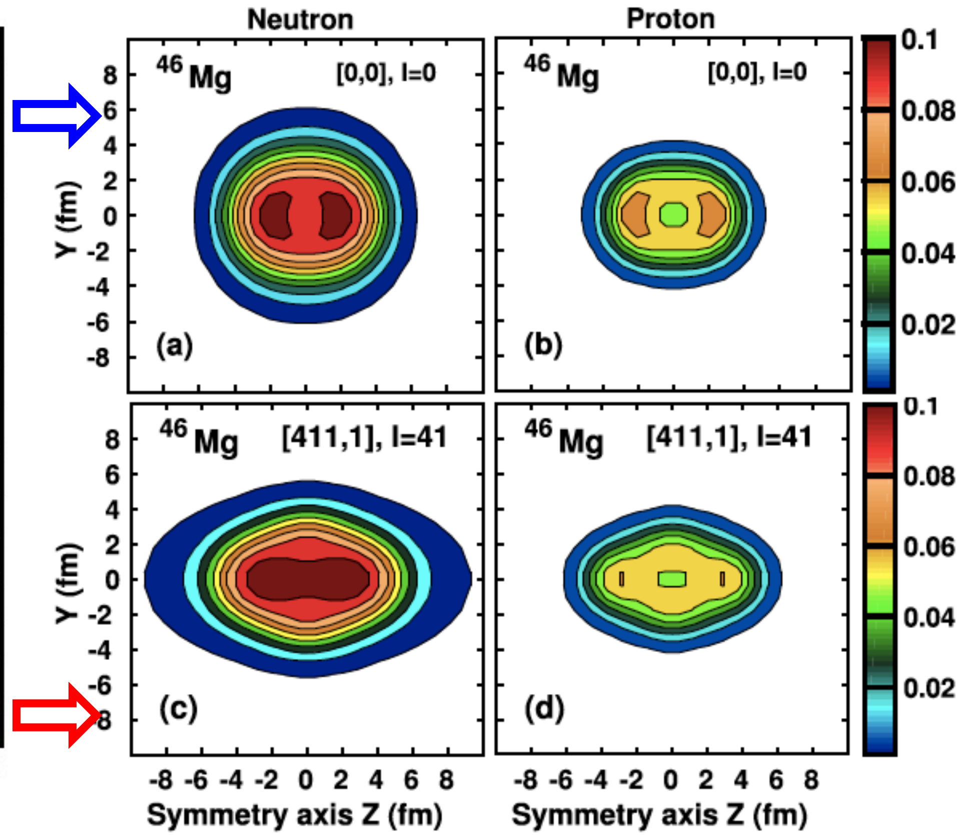

AA, N. Itagaki, D. Ray, PLB 794 (2019) 7

Density distributions

Modification of proton and neutron density distributions by means of particle-hole excitations

The birth of particle-bound rotational bands: a tool for an extension of nuclear landscape towards higher neutron number

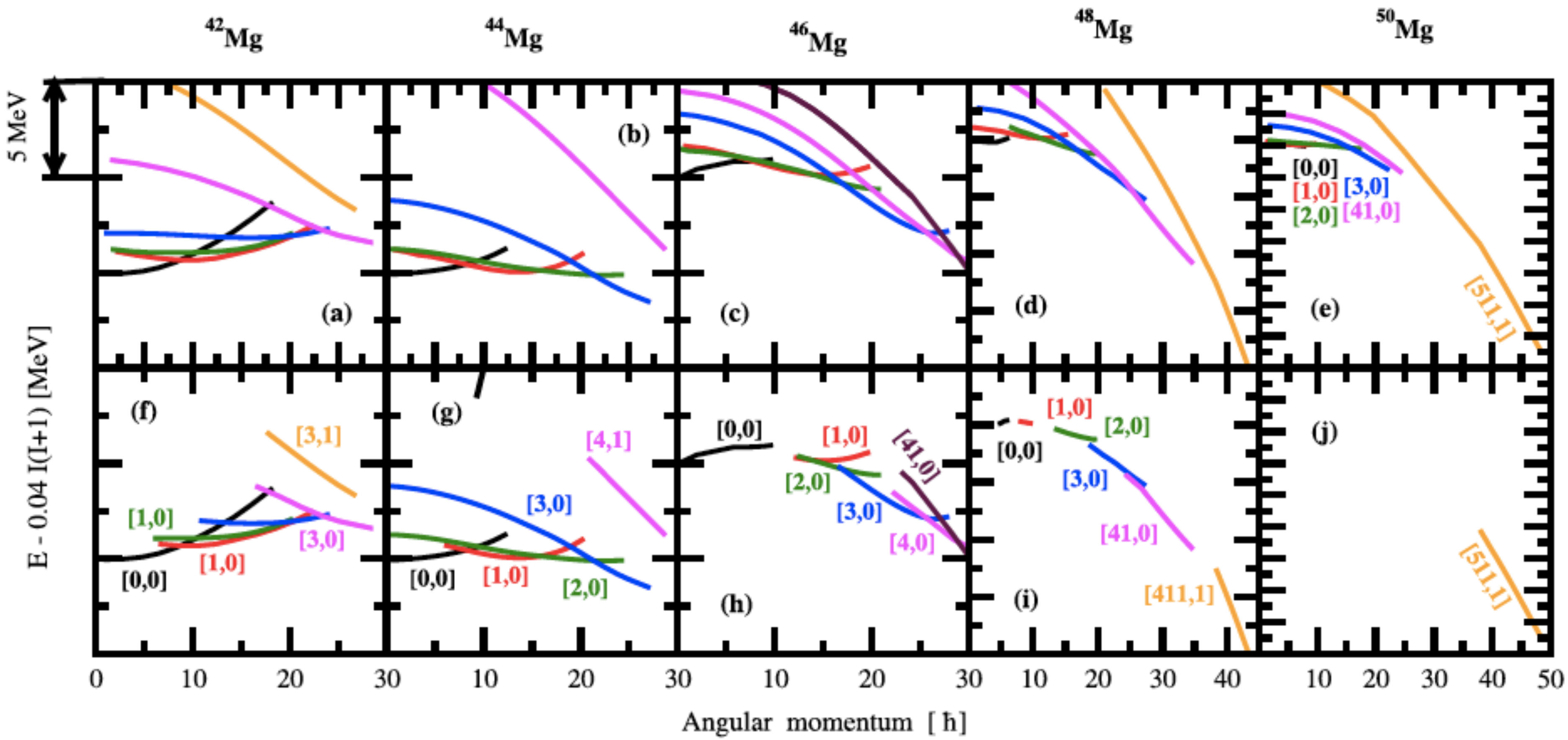

Last neutron bound nucleus at spin I=0 = spin zero neutron drip line

AA, N. Itagaki, D. Ray, PLB 794 (2019) 7

The origin of new phenomenon: the birth of particle-bound rotational bands in proton-rich nuclei

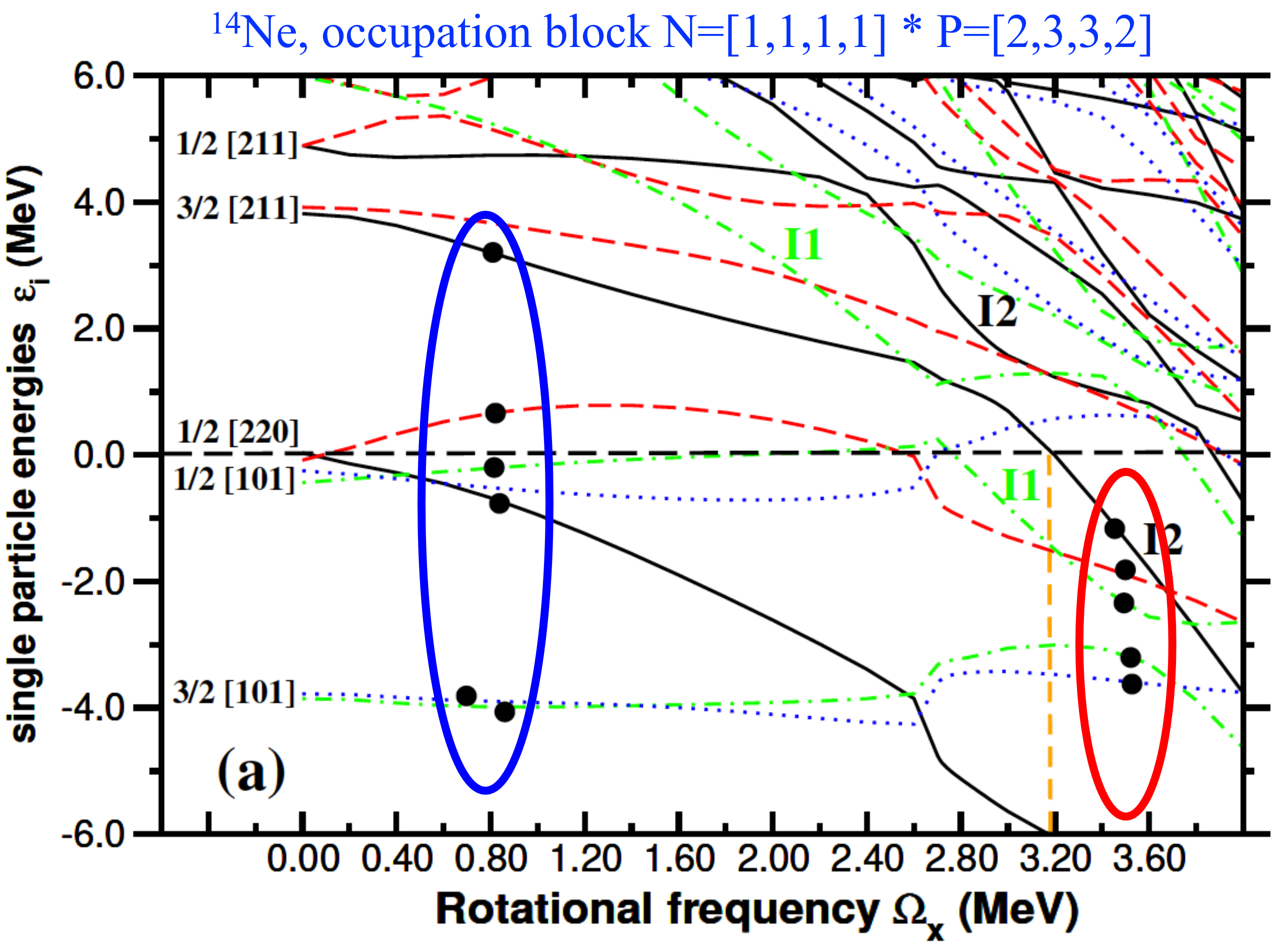

Fast rotation and multiply particle-hole excitations are expected to kill static pairing and thus the coupling with continuum.

S.Teeti, AA, A.Taninah, submitted to PRC

Intruder orbitals I* = extremely mixed wavefunctions. For example, at frequency 3.2 MeV the squared weights of the N = 2, 4, 6, and 8 shells in the structure of the wave function of the intruder orbital I2 of the configuration [0, M2] are 0.09, 0.12, 0.19 and 0.21, respectively.

New phenomenon: the birth of particle-bound rotational bands in proton-rich nuclei

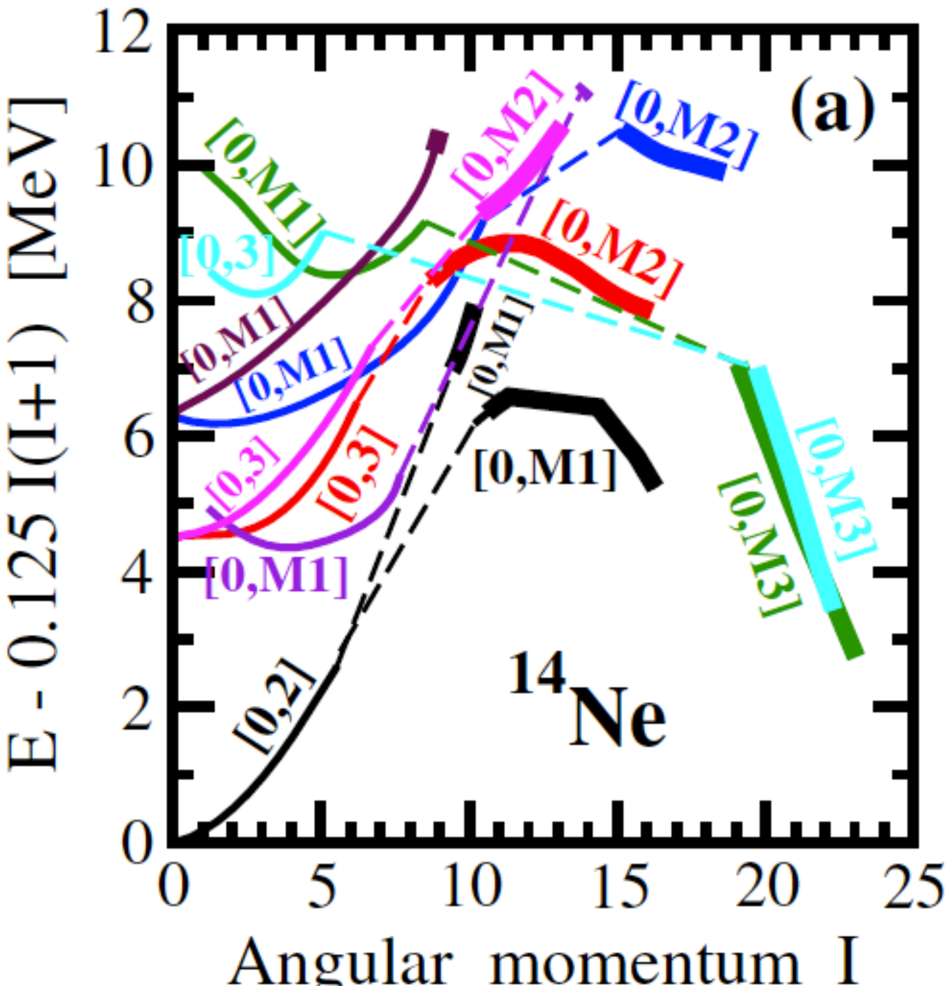

Thin solid lines – proton unbound parts of rotational bands

Thick solid line – proton bound parts of rotational bands

Dashed lines connect these parts

Configuration labels:

- [n,p] = n(p) indicates the number of occupied neutron(proton) intruder orbitals. Depends on mass region: in ^{14}Ne, intruders are from the N=2 shell.
- the label “M#” is used in shorthand label [n,p] to indicate strongly mixed orbitals (M) and their number #.

New phenomenon: rotation-induced giant proton halo

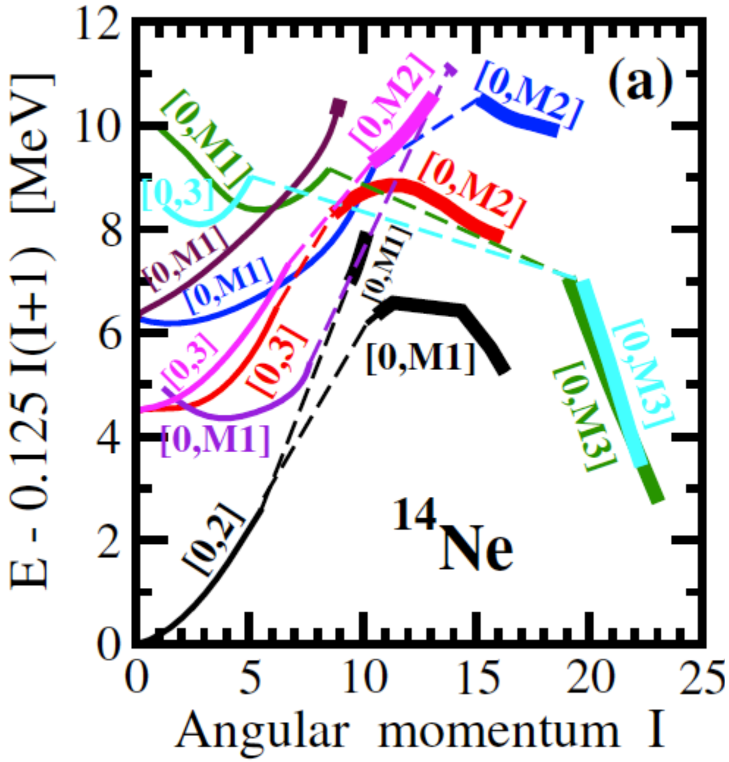

S.Teeti, AA, A.Taninah, submitted to PRC

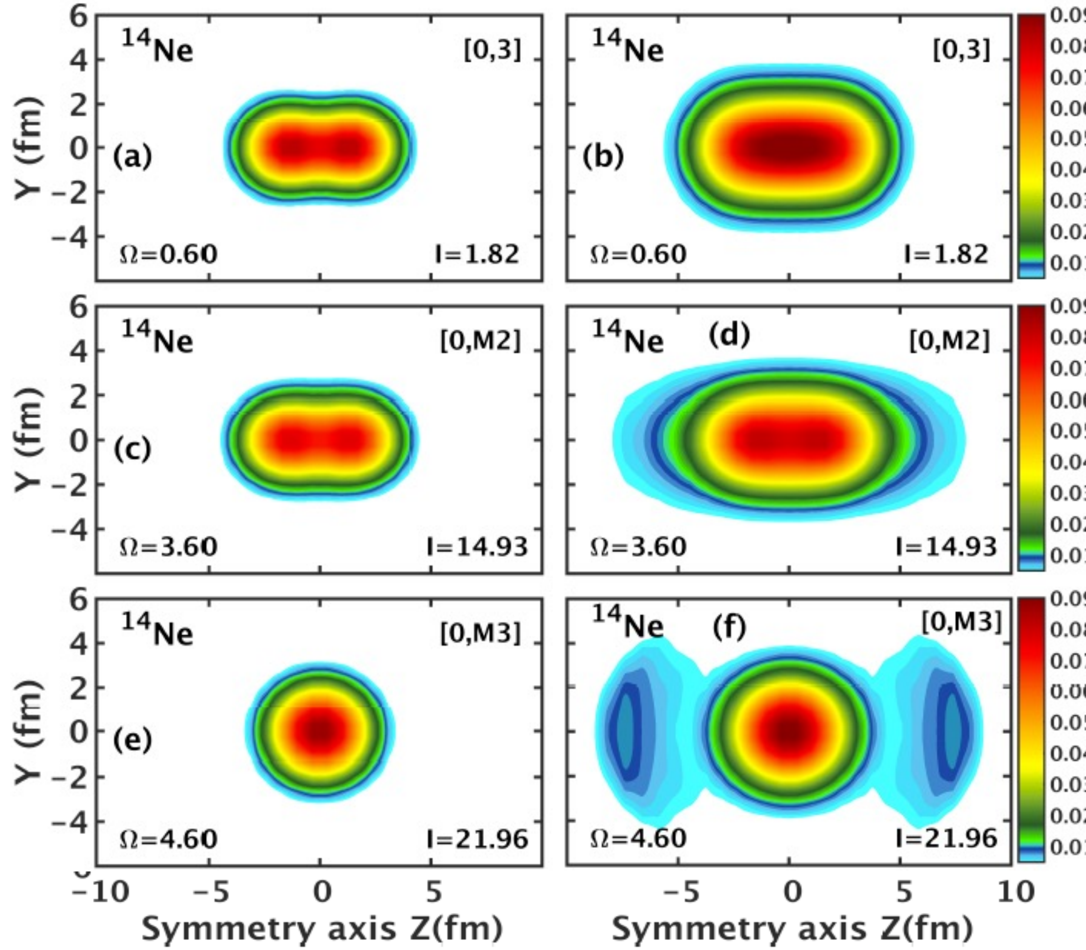

Mechanism of formation: occupation of strongly mixed M-orbitals

Completely different from the one in non-rotating nuclei in which proton halo is formed due to the occupation of loosely bound *s* and *p* orbitals

Ne isotopic chain: from two-proton drip line to more proton-rich nuclei

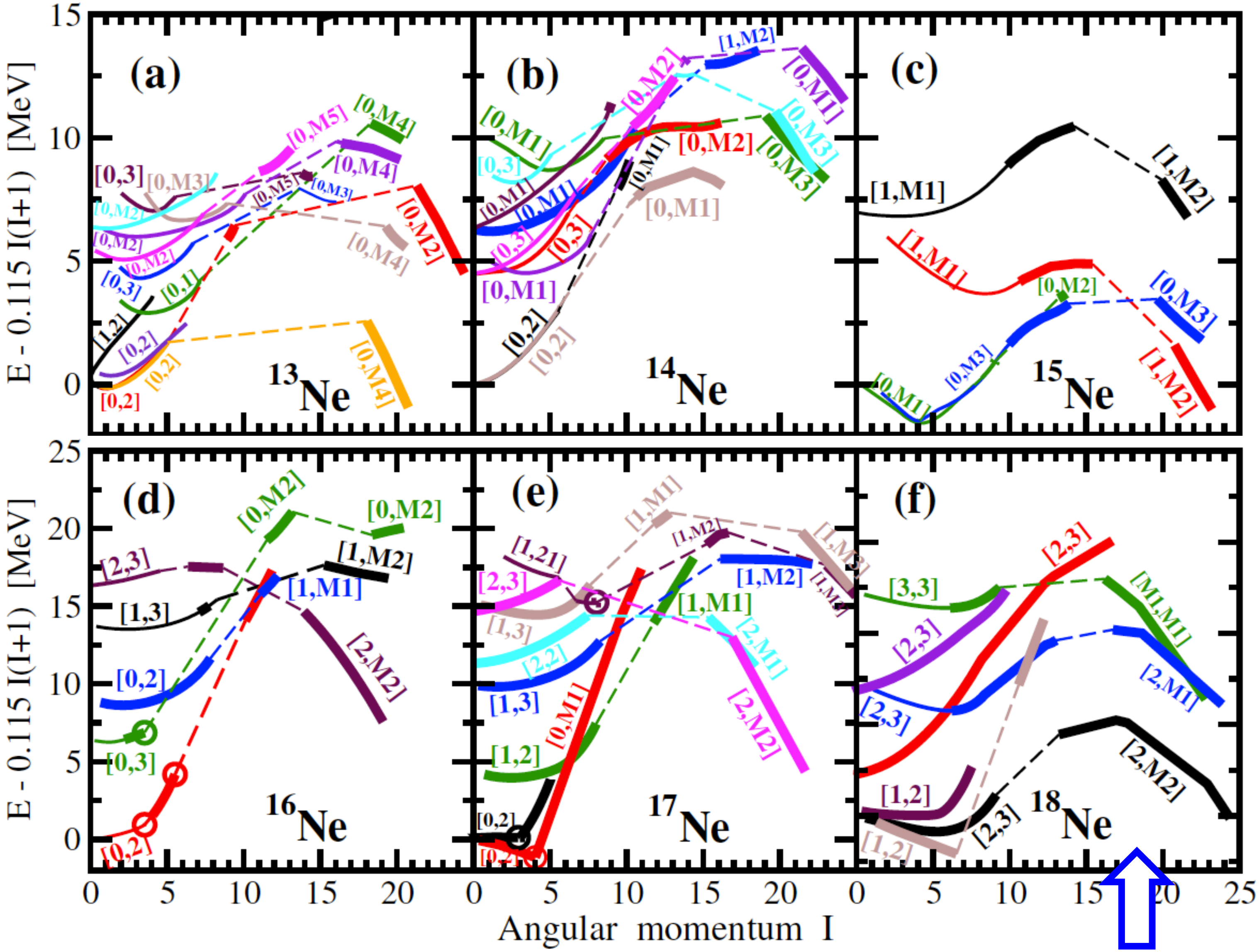

S.Teeti, AA, A.Taninah, in preparation

^{18}Ne = last proton bound nucleus at spin I=0

Giant proton halos in the high-spin configurations of the nuclei bound at spin I=0

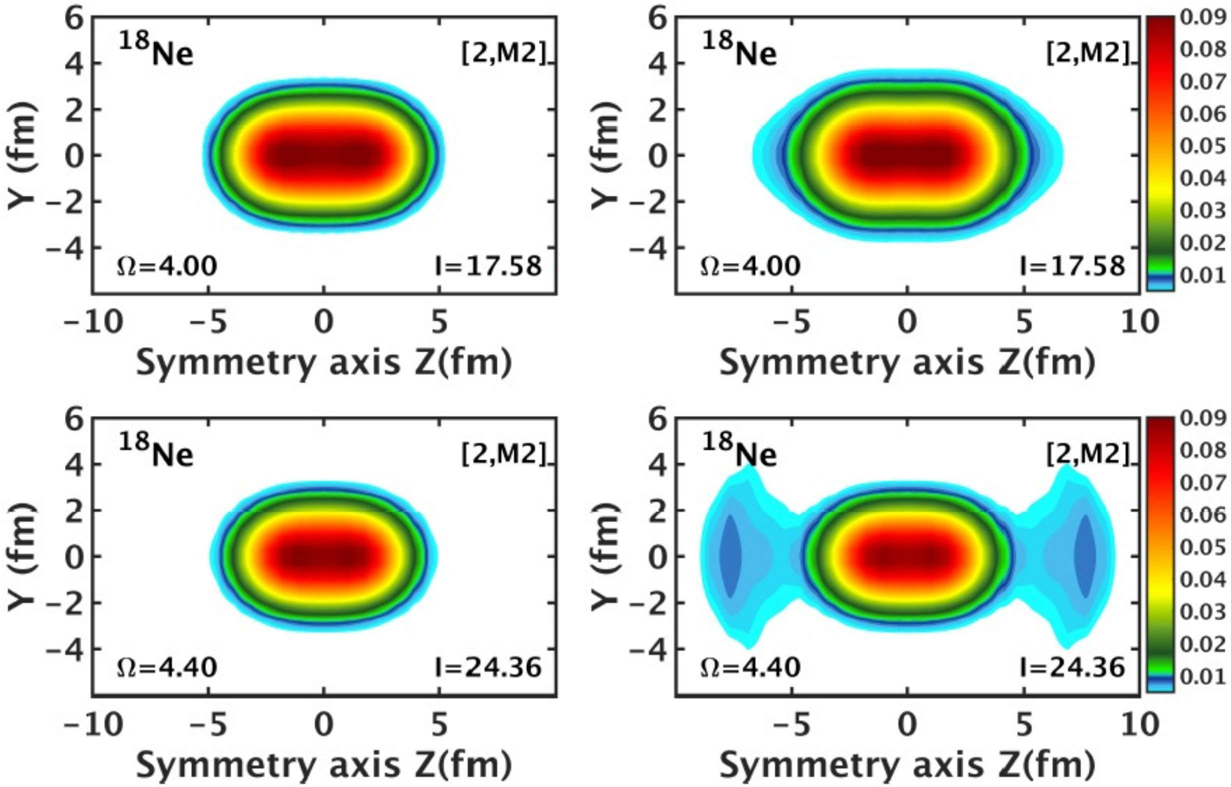

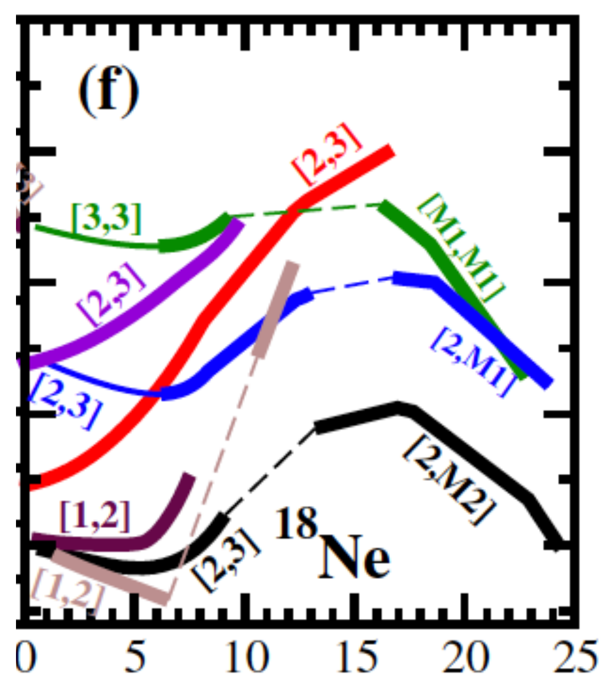

S.Teeti, AA, A.Taninah, in preparation

Some samples of exotic nuclear shapes in proton-bound parts of rotational bands

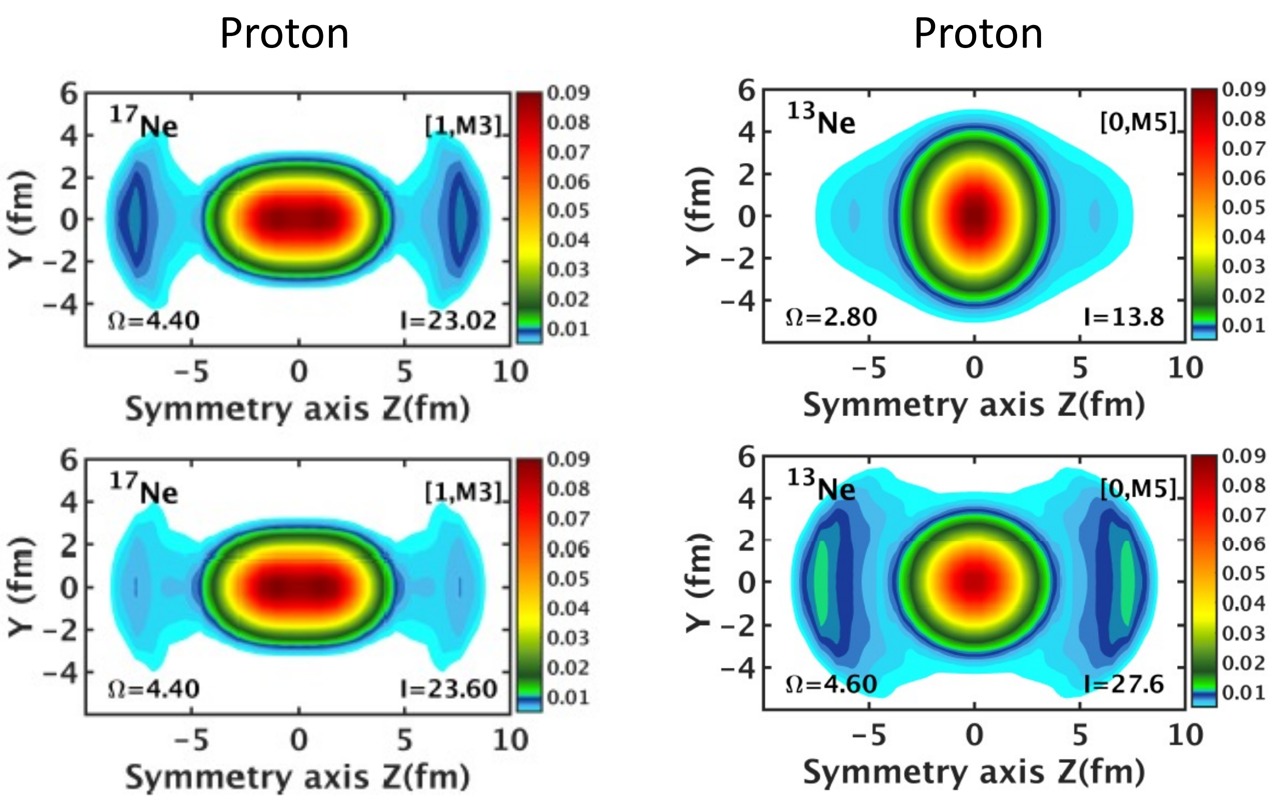

S.Teeti, AA, A.Taninah,
in preparation

The absence of giant proton halos in high-Z (Z>20) nuclei

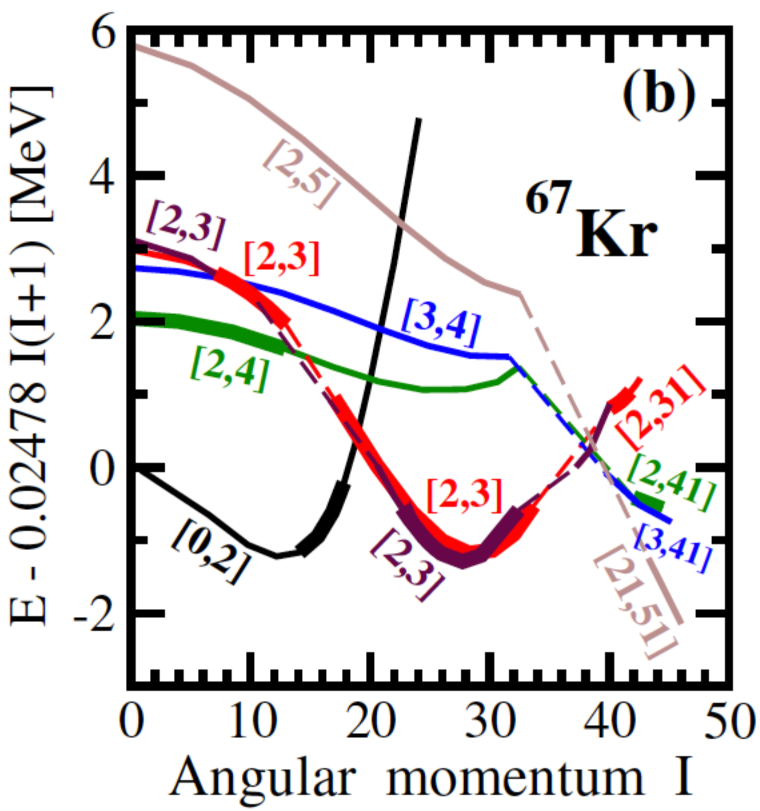

Configurations are labeled by shorthand labels [n; p1p2] where n (p1p2) indicate the number of the occupied N = 4 neutron (n) orbitals and N = 4 (p1) and N = 5 (p2) proton orbitals. The label p2 is omitted when p2 = 0.

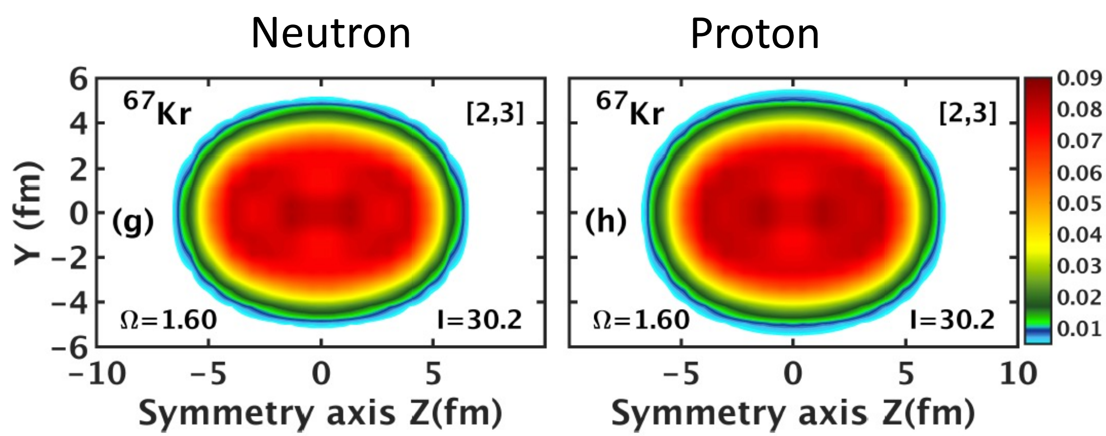

some excited configurations can be proton-bound at very low spin in contrast to the proton unbound ground state rotational bands.

S.Teeti, AA, A.Taninah, submitted to PRC

The extension of particle-bound nuclear landscape beyond spin-zero proton drip line.

Dashed filling pattern – nuclei in which giant proton halos appear

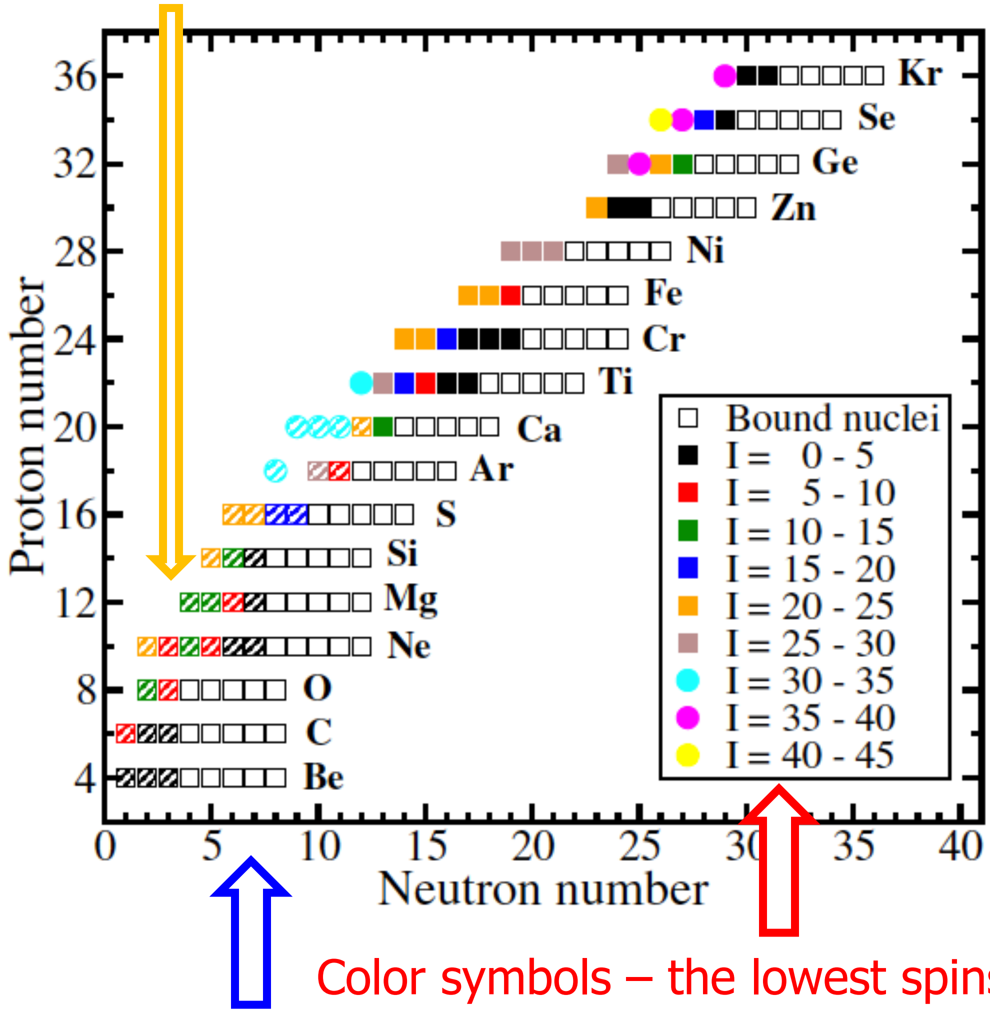

For many nuclei located beyond spin zero proton-drip line the transition to proton-bound configurations is seen at relatively modest spin values.

With increasing proton excess the transition appear at higher spin values.

Giant proton halos are suppressed in high Z nuclei.

Color symbols – the lowest spins at which proton bound rotational bands appear

Open squares – proton bound nuclei at spin I=0

S.Teeti, AA, A.Taninah, submitted to PRC

Conclusions

1. The increase of proton number Z beyond Z~130 triggers the demise of ellipsoidal/spheroidal nuclear shapes and transition to toroidal shapes. The only exception are three regions of “excited” spherical shapes which are potentially relatively stable; they become the ground states if respective toroidal shapes are unstable.

2. The birth of particle-bound rotational bands is predicted in the nuclei near drip lines. It manifest the transition to particle-bound part of rotational band from particle-unbound part [resonance part in neutron-rich nuclei or proton-emitting part in proton-rich nuclei] triggered by strong Coriolis force acting upon occupied orbitals. This allows to extend nuclear landscape at non-zero spin beyond the boundaries defined at spin zero.

This material is based upon work supported by the U.S. Department of Energy, Office of Science, Office of Nuclear Physics under Award No. DE-SC0013037.